JOURNAL OF RAMAN SPECTROSCOPY, VOL. 21, 103–107 (1990)

Raman Spectra of Tetramethylammonium–Trimethylammonium Mixed Ion Vermiculite Clay Intercalation Compounds

S. A. Solin† and H. X. Jiang
Department of Physics and Astronomy, Center for Fundamental Materials Research, Michigan State University, East Lansing, Michigan 48824-1116, USA

H. Kim and T. J. Pinnavaia
Department of Chemistry, Center for Fundamental Materials Research, Michigan State University, East Lansing, Michigan 48824-1116, USA

The composition dependence of the Raman spectra of the mixed ion vermiculites $[(CH_3)_4N^+]_{1-x}[(CH_3)_3NH^+]_x$–V (V = vermiculite) have been studied in the range $0 \leqslant x \leqslant 1$. The torsional mode frequencies exhibit a small shift (*ca.* 2 cm^{-1}) to lower energy with increasing x and their composition dependence is distinct from that shown by the corresponding modes of $Cs_{1-x}Rb_x$–V. These differences are attributed to a variation of the guest–host force constants and in particular to the interactions between the guest ions and the basal oxygens, which depend strongly on the size difference, ΔD, between the guest ion pairs. Using a van der Waals-type force model and the nearest neighbor approximation, the torsional mode frequencies of the pure end-member compounds of the two mixed ion systems discussed above have been successfully accounted for.

INTRODUCTION

Clay intercalation compounds (CICs) have recently attracted interest in solid-state physics because of their interesting physical properties.[1–3] One of the most important features of CICs is that they can be used as an ideal quasi-two-dimensional (2D) system with which to investigate 2D physical and chemical processes. These solids exhibit unique structures,[4,5] in which multilayers of guests can intercalate monolayers of host. They are therefore a novel class of quasi-two-dimensional material and have many advantages for physics investigations. For instance, CICs are ideal systems to study the 2D percolation process because one can accurately control (to 1 part in 10^5–10^6) the number of 'bonds' by controlling the concentration x ($0 \leqslant x \leqslant 1$) in a compound such as $A_{1-x}B_x$–V [V = vermiculite, $A = (CH_3)_4N^+$ and $B = (CH_3)_3NH^+$ in this paper]. This control is especially important near the percolation threshold[6] where fractals[7] dominate the structural arrangement of the intercalated species. Such control is not readily obtained with other types of intercalated lamellar solids. Although clays and CICs have been studied for many years by geologists, chemists, soil scientists, etc.,[8] the above-described novel properties have only recently stimulated attention in the solid-state physics community.

Vermiculite, the host system of interest here, is a specific example of a trioctahedral 2:1 layered silicate.[4,5] Its negatively charged layers are formed from a sheet of edge connected octahedra (M^{VI} = Mg, Al, Fe) which is symmetrically bound to two sheets of corner connected tetrahedra (M^{IV} = Si, Al) as shown in Fig. 1. The layers of oxygen atoms which terminate the clay layers are arranged in a Kagomé lattice whose hexagonal pockets form a triangular lattice of gallery sites. Overall charge neutrality of the clay system is derived from the presence of intragallery cations which can be readily exchanged with other cations in the 'intercalation' process. In the interlayer galleries of vermiculite and other clays chemical reactions can be selective, specific and distinct compared with the corresponding reaction in the free space.[9] The range of stability, structure and other physical properties depends not only on the type of exchange cation that occupies the interlayer gallery,

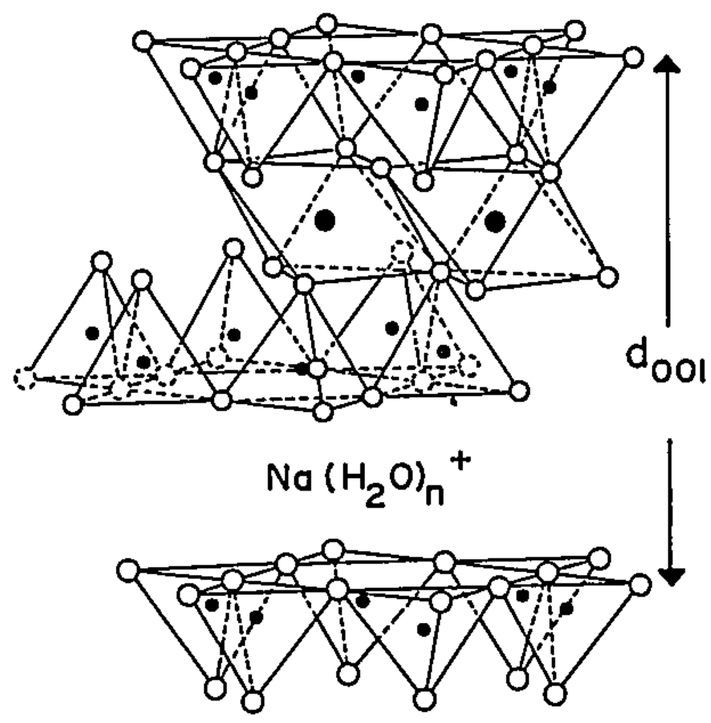

Figure 1. Schematic illustration of the tetrahedral and octahedral sites in a 2:1 layered silicate. Open circles are oxygen, closed circles are cations in tetrahedral (Si, Al) and octahedral (Al, Fe, Mg, Li) positions. Hydroxyl groups (not distinguished from oxygen) are located in the second and third basal planes of oxygens.

† Present address: NEC Research Institute, Princeton, NJ 08540, USA

0377-0486/90/020103–05 $05.00

Received 21 August 1989
Accepted 25 September 1989

but also on the intrinsic composition and properties of the silicate layer itself.

For the ternary CICs $A_{1-x}B_x$–V, it is important to understand the physical properties as a function of composition, x. This understanding reveals the fundamental aspects of interactions between ions A and B (guest–guest interactions) and between ions A (or B) with and basal oxygens of the host clay layers (guest–host interactions). Additional important properties of a ternary CIC are the x dependence of layer rigidity, the structure (such as basal spacing) and the distributions of A and B ions in the galleries, all of which are heavily influenced by the guest–guest and guest–host force constants. Extensive work on graphite intercalation compounds[10,11] and other layered solids has shown that Raman spectroscopy is an effective tool with which to study these force constants. Accordingly, we report in this paper the application of this technique to the $[(CH_3)_4N^+]_{1-x}[(CH_3)_3NH^+]_x$–V system.

The x dependence of the Raman spectra of a related system, $Cs_{1-x}Rb_x$–V, has been studied previously.[1] Of particular interest was the host layer torsional mode, whose eigenvector is shown schematically in the inset in Fig. 2. The frequency of that mode showed a continuous nonlinear shift to low energy as x increased from 0 to 1. This behaviour has been qualitatively attributed to force constant variations which result from the different degree to which the Rb and Cs cations are 'enveloped' by the hexagonal oxygen cavities of the bounding clay layers. The nonlinear shift in torsional mode frequency of $Cs_{1-x}Rb_x$–V has also been calculated quantitatively by Gupta *et al.*,[12] who used an angular force model and the virtual crystal approximation. Their calculation elucidated the mechanism for the intrasystem nonlinear x dependence of the torsional mode of $Cs_{1-x}Rb_x$–V. In this paper, we present the results for the composition dependence of the torsional Raman mode of $[(CH_3)_4N^+]_{1-x}[(CH_3)_3NH^+]_x$–V in the range $0 \leqslant x \leqslant 1$. In an effort to understand the intersystem properties of vermiculite-based CICs, our results are compared with those for $Cs_{1-x}Rb_x$–V.[1] The distinct behaviors of the torsional mode in these two systems suggests the important role of the relative cation sizes r_A/r_B and size difference $r_A - r_B$ (where r is the radius of the ion), since these parameters of are very different for $[(CH_3)_4N^+]_{1-x}[(CH_3)_3NH^+]_x$–V and $Cs_{1-x}Rb_x$–V. The different force constants between guest ions and the basal oxygens also plays an important role. To probe this role quantitatively we used a van der Waals force model and the nearest neighbor approximation to account successfully for the torsional mode frequencies of the pure end-member compounds of the two mixed ion systems.

EXPERIMENTAL

$[(CH_3)_4N^+]_{1-x}[(CH_3)_3NH^+]_x$–V was prepared from Mg–V using an ion-exchange method.[13] The samples were made of powder in which each crystallite was a few micrometers in diameter. The samples are well ordered and water free. Highly oriented films were prepared from powdered natural vermiculite by first ion exchanging with $(CH_3)_3NH^+$ in the presence of EDTA anion and subsequently exchanging with $(CH_3)_4N^+$ by adding $(CH_3)_3NH^+$ salt solution containing the desired relative concentrations of $(CH_3)_4N^+$ to the salt-free $(CH_3)_3NH^+$–V suspension. The water was removed by heating the samples in an oven for 12 h at 100 °C. Film samples formed on glass slides exhibited mosaic spreads of $\Omega \approx 5°$,[2] indicating an oriented morphology with the silicate layers parallel to the slide surface. The x values were determined by a titration method in which the $[(CH_3)_4N^+]_{1-x}[(CH_3)_3NH^+]_x$–V was treated with NaOH solution and liberated $(CH_3)_4N^+$ was distilled and titrated with standard HCl. Available interlayer lattice sites within a given gallery are randomly occupied by the $(CH_3)_4N^+$ and $(CH_3)_3NH^+$ ions and the average cell composition[4] is $\{[(CH_3)_4N^+]_{1-x}\ [(CH_3)_3NH^+]_x\}_{1.72}\ (Si_{5.87}Al_{2.13})[Mg_{5.25}Al_{0.48}]O_{20}(OH)_4(zH_2O)$ where z is a small number after water is removed.

Raman spectra were measured using the 514.5-nm line of an argon ion laser at typical power levels of 150 mW, a Spex 1402 double spectrometer and a photon counting detection system. All measurements were made with the scattered light collected at 90° to the direction of propagation of the laser light which was incident at an angle about 45° to the sample plane and polarized in the plane of incidence. The data were taken at room temperature and the polarization of the scattered light was not analyzed.

RESULTS

Typical room-temperature Raman spectra for the low-frequency vibrations of $[(CH_3)_4N^+]_{1-x}[(CH_3)_3NH^+]_x$–V are shown for five different compositions of x in Fig. 2. The torsional mode, whose frequency and eigenvector are well known from the calculations of Ishii *et al.*[14] and Gupta *et al.*,[12] occurs at

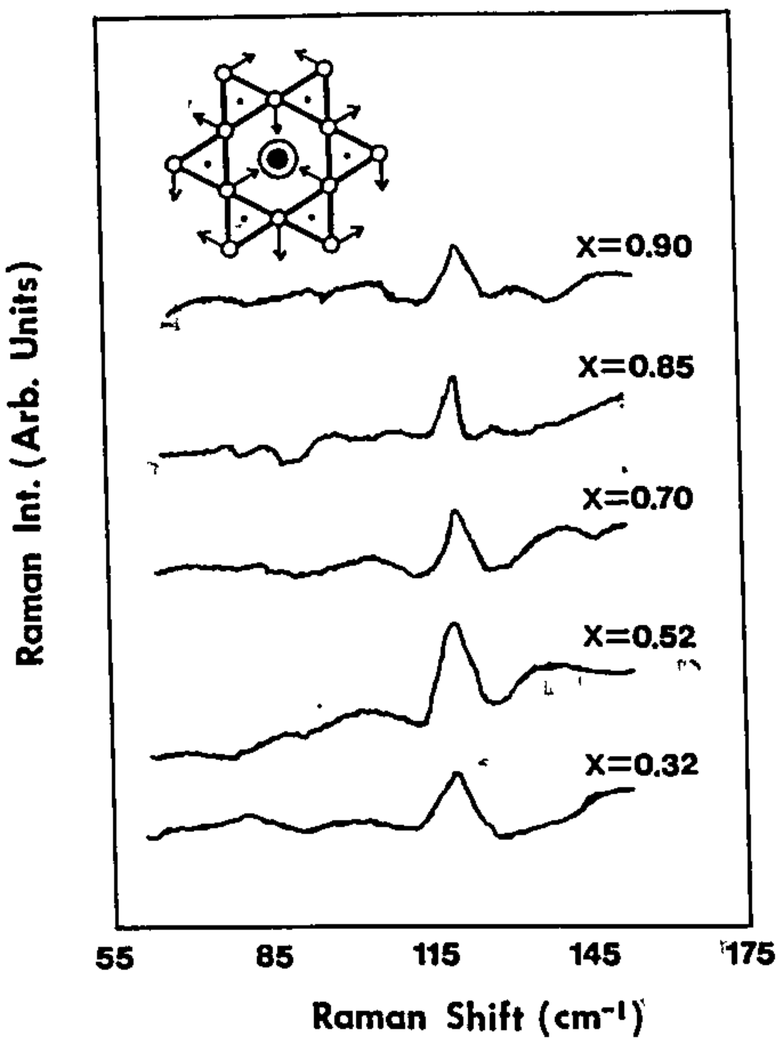

Figure 2. Raman spectra of the low-frequency vibrations of $[(CH_3)_4N^+]_{1-x}[(CH_3)_3NH^+]_x$–V for five different compositions of x. Inset: the vermiculite structure viewed along the c-axis showing oxygen (○), Si or Al (●) and $[(CH_3)_4N^+]$ or $[(CH_3)_3NH^+]$ (⊙).

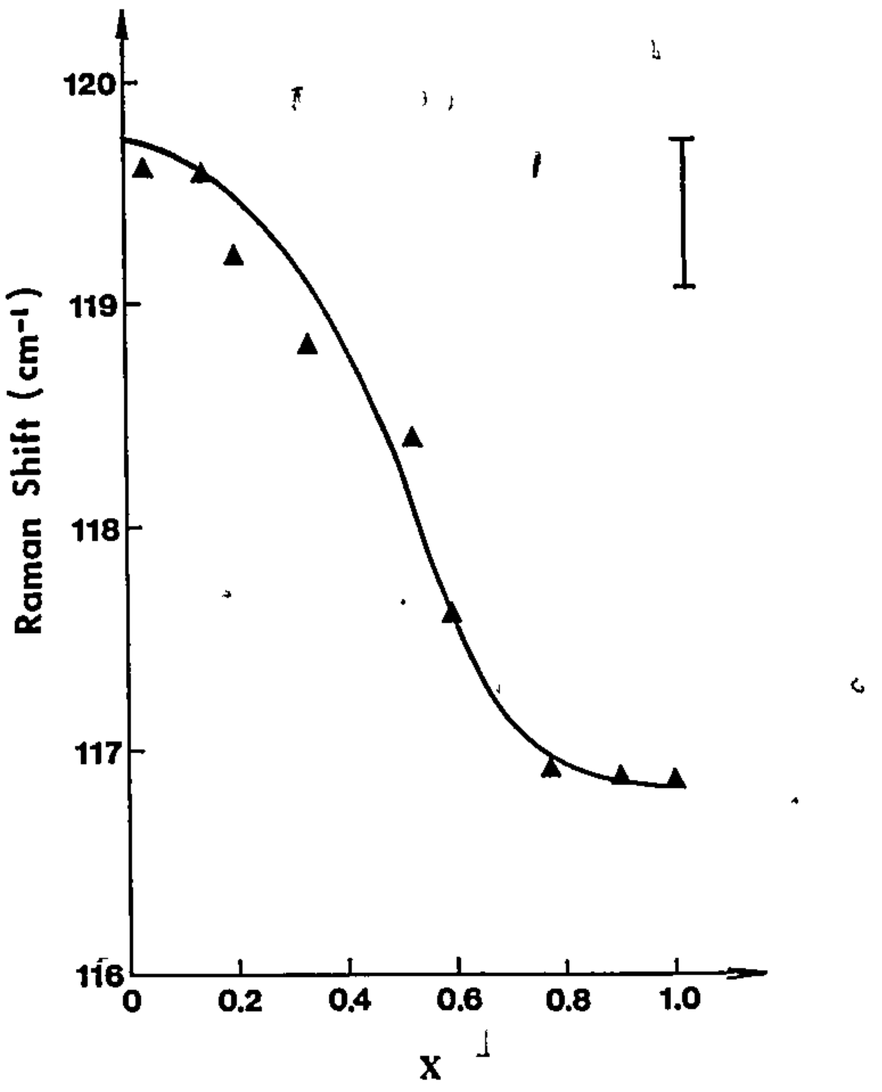

Figure 3. x Dependence of the Raman shift of the torsional mode of $[(CH_3)_4N^+]_{1-x}[(CH_3)_3NH^+]_x$–V. The line in the figure is a guide to the eye. The error bar is indicated on the right.

about 118 cm^{-1}. A few other high-frequency modes have also been observed which correspond to intralayer modes of the host layer. These high-frequency modes will not be discussed here. The focus of this paper is the broad 118 cm^{-1} A'' interlayer mode. In the inset in Fig. 2, we show the vermiculite structure viewed along the c-axis and the oxygen (○), Si or Al (●) and $[(CH_3)_4N^+]$ or $[(CH_3)_3NH^+]$ ions (⊙). The arrows indicate the eigenvector of this torsional A'' mode.[1] This mode is identified on the basis of its energy,[15] x dependence and the correspondence with $Cs_{1-x}Rb_x$–V. On comparison with $Cs_{1-x}Rb_x$–V, the torsional mode frequency of $[(CH_3)_4N^+]_{1-x}[(CH_3)_3NH^+]_x$–V shifts to high energy (from 106 to about 118 cm^{-1}). This shift is caused by two effects. First, the interactions between $(CH_3)_4N^+$ and $(CH_3)_3NH^+$ and the basal oxygens of the host clay are stronger than those of Cs and Rb. Second, the $(CH_3)_4N^+$ and $(CH_3)_3NH^+$ ions are larger than Cs and Rb; this increases the basal spacing d. The torsional mode frequencies are mainly determined by these two parameters. As the x value increases, the torsional mode frequency of $[(CH_3)_4N^+]_{1-x}[(CH_3)_3NH^+]_x$–V shifts nonlinearly to low frequency in a manner similar to that of $Cs_{1-x}Rb_x$–V.[1]

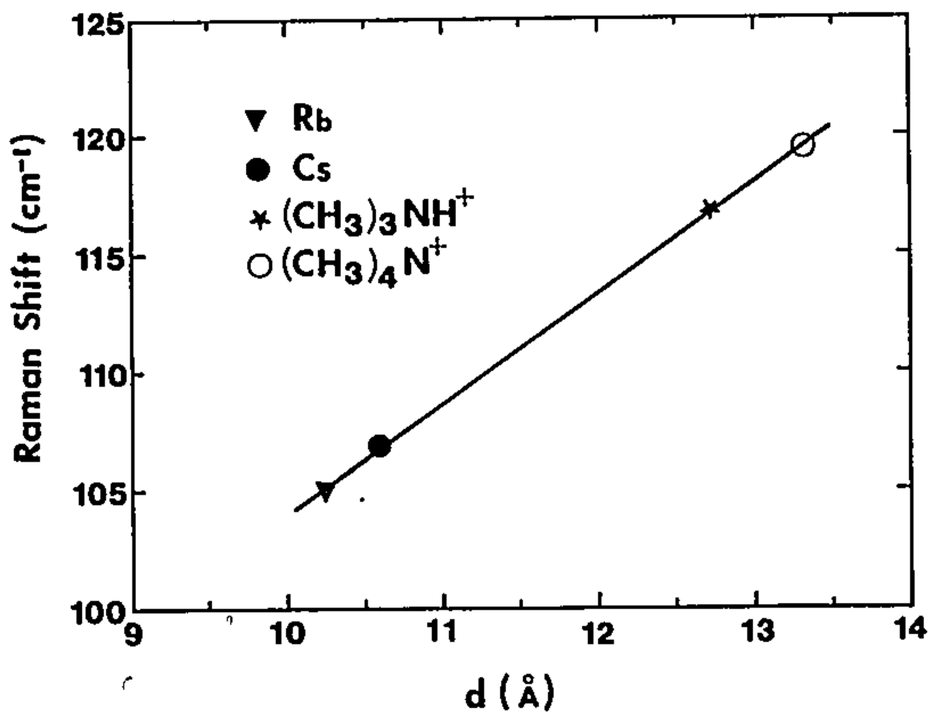

Figure 4. Raman shift of the torsional mode as a function of basal spacing d for M^+–V, where $M^+ = Rb^+$, Cs^+, $(CH_3)_3NH^+$ and $(CH_3)_4N^+$. The basal spacings d were obtained from x-ray experiments.[1,2]

The x dependence of the torsional mode frequency of $[(CH_3)_4N^+]_{1-x}[(CH_3)_3NH^+]_x$–V is plotted in Fig. 3. The line in the figure is a guide to the eye. The error bar is shown on the right. It can be seen that at the two ends ($x \approx 0$ or $x \approx 1$), there is minimal shift as the composition x changes while the frequency shifts almost linearly with x in the region $0.2 \leqslant x \leqslant 0.6$. This behavior of the torsional mode of $[(CH_3)_4N^+]_{1-x}[(CH_3)_3NH^+]_x$–V is distinct from that shown by the corresponding mode of $Cs_{1-x}Rb_x$–V, where the frequency shift is highly nonlinear throughout the entire range of x. We cannot at present account quantitatively for the frequency dependence exhibited in Fig. 3 (see Ref. 12 for a discussion of the x dependence of the Raman frequency of the torsional mode of $Cs_{1-x}Rb_x$–V).

Although Fig. 3 shows the x dependence of the Raman shift of the torsional mode of $[(CH_3)_4N^+]_{1-x}[(CH_3)_3NH^+]_x$–V, the Raman shift of the torsional mode as a function of basal spacing d is more fundamental, since these two should be connected directly. For mixed ion vermiculite CICs with known force constants, the frequency of the torsional mode should be uniquely determined by the basal spacing d and the relationship between them can be calculated. The basal spacing of $[(CH_3)_4N^+]_{1-x}[(CH_3)_3NH^+]_x$–V has been previously determined for $0 \leqslant x \leqslant 1$ from x-ray measurements.[2] By combining the data in Fig. 3 with the x-ray results for the end-member compounds, $x = 0$ and $x = 1$, and the corresponding results for $Cs_{1-x}Rb_x$–V, we have deduced the Raman shift as a function of d for M^+–V with $M^+ = Rb^+$, Cs^+, $(CH_3)_3NH^+$ and $(CH_3)_4N^+$. The resulting intersystem plot, which shows a linear relationship between the torsional mode Raman shift and basal spacing, is presented in Fig. 4.

We have concentrated on the end-member compounds in this discussion because they possess a spatially homogeneous environment that determines the basal spacing and force constants. In contrast, in the mixed ion systems with $0 < x < 1$ there are spatial fluctuations in the local environment. Hence the interatomic forces and gallery height can vary significantly from site to site within a given interlayer space. Although there are well established methods for treating such variations, e.g. the virtual crystal approximation, we feel that in this initial attempt to understand intersystem effects it would be prudent to avoid the complications attendant on spatial fluctuations.

CALCULATION

In this section, we present a calculation of the Raman frequency of the torsional mode of a binary vermiculite system, i.e. one which contains a single type of cation in the gallery. There are two assumptions in this calculation. First, we assume that the interactions between the oxygen–oxygen and oxygen–guest ion are molecular so that they are well described by a van der Waals type force.[16] Second, we assume that the guest ions are

located in the centers of the hexagonal pockets of the Kagomé lattice of the bounding oxygen planes. This should be true if we consider the minimum energy of the system or the equilibrium position of the guest ions. Under these two assumptions, the positions of the oxygen atoms and of the guest ions are all known explicitly. One should note that when the system vibrates in the torsional mode, the position of each oxygen atom in the basal plane is also determined uniquely, since we know the eigenvector of the mode (guest ions are motionless in the torsional mode).

Figure 5 shows the configuration of oxygen atoms and guest ions of $A_{1-x}B_x$–V viewed in the direction (a) along and (b) perpendicular to the c-axis with lattice parameter $b = 2.67$ Å. The arrows in Fig. 5(a) indicate the distorted positions of oxygen atoms in the torsional mode. Note that the distortions for the positions of each of the oxygen atoms are equal. We concentrate on the vibrational motion of the oxygen atom labeled 1 since the vibrations of other oxygen atoms are identical. We only show the nearest neighbors of oxygen atoms, as we shall use the nearest neighbor approximation later. X and Y are two axes in the cartesian coordinate system. The guest ions are located at a height h above (or below) the basal plane, as shown in Fig. 5(b), where d is the basal spacing which was measured in an x-ray experiment.[2] The thickness of the silicate layer is 9.34 Å.[1] From the known diameter of the oxygen atom (2.92 Å),[17] the distance between the top and bottom of the silicate layers can be determined and is 6.42 Å. Consequently, the distance between the center of the guest ion and the basal plane is $h = (d - 6.42)/2$ (Å). From these parameters and Fig. 5, we can write the relative distance of the six nearest neighbors to the oxygen atom 1 in the torsional mode vibration as $\mathbf{R}_{i1} = x_{i1}\mathbf{i} + y_{i1}\mathbf{j} + z_{i1}\mathbf{k}$, which can be written in shortened form as $[x_{i1}, y_{i1}, z_{i1}]$. Then we have

$$\mathbf{R}_{21} = [(\sqrt{3}/2)(b + \delta), (-1/2)(b - 3\delta), 0]$$
$$\mathbf{R}_{31} = [(-\sqrt{3}/2)(b + \delta), (-1/2)(b - 3\delta), 0]$$
$$\mathbf{R}_{41} = [(\sqrt{3}/2)(b - \delta), (1/2)(b + 3\delta), 0]$$
$$\mathbf{R}_{51} = [(-\sqrt{3}/2)(b - \delta), (1/2)(b + 3\delta), 0]$$
$$\mathbf{R}_{61} = [0, b + \delta, h]$$
$$\mathbf{R}_{71} = 0, \delta - b, h]$$

where δ is the distortion of oxygens.

Assuming that the forces between oxygen–oxygen and oxygen–guest ion have the following form:

$$\mathbf{F}_{i1} \propto R_{i1}^n(\mathbf{R}_{i1}/|\mathbf{R}_{i1}|), \qquad i = 2, 3, \ldots, 7 \tag{1}$$

the total force acting on the oxygen atom 1 can be written as

$$\mathbf{F}_t = \sum_{i=2}^{\infty} \eta' R_{i1}^n(\mathbf{R}_{i1}/|\mathbf{R}_{i1}|) = \sum_{i=2}^{7} \eta' R_{i1}^n(\mathbf{R}_{i1}/|\mathbf{R}_{i1}|) \tag{2}$$

where

$$\eta' = \begin{cases} \alpha, & i = 2, 3, 4, 5, \quad \text{(oxygen–oxygen)} \\ \beta, & i = 6, 7, \quad \text{(oxygen–guest ion)} \end{cases} \tag{3}$$

and α, $\beta < 0$ correspond to the attractive force constants between oxygen–oxygen and oxygen–guest ion. The parameter β will be different with different binary CICs. In Eqn (2), we have used the nearest neighbor approximation and there is a total of six nearest neighbors for each oxygen in the basal plane. The total force acting on the oxygen atom 1 in the y direction which determines the vibration frequency is (to first order in δ)

$$F_y = \sum_{i=2}^{7} F_{i1,y} = 2b^{n-1} \times \{3\alpha + \beta(1 + h^2/b^2)^{(n-3)/2}(n + h^2/b^2)\}\delta \tag{4}$$

Also, we have

$$F_y = m\ddot{\delta} \tag{5}$$

where m is the mass of the oxygen atom. From Eqns (4) and (5), we have

$$\omega^2 = (-2b^{n-1}/m) \times [3\alpha + \beta(1 + h^2/b^2)^{(n-3)/2}(n + h^2/b^2)] \tag{6}$$

The relationship between the vibration frequency of the oxygens, ω, and the Raman shift of the torsional mode, $\tilde{\nu}$, is

$$\omega = 2\pi c\tilde{\nu} \tag{7}$$

From Eqns (6) and (7), we finally obtain

$$\tilde{\nu}^2 = (-2b^{n-1}/m)(\alpha/4\pi^2c^2) \times [3 + \gamma(1 + h^2/b^2)^{(n-3)/2}(n + h^2/b^2)] \tag{8}$$

where $\gamma = \beta/\alpha$ is the ratio of force constants between oxygen–guest ion to oxygen–oxygen.

Equation (8) connects the Raman shift of the torsional mode with the physical parameters of M^+–V. From the parameters b, h and m and the experimental

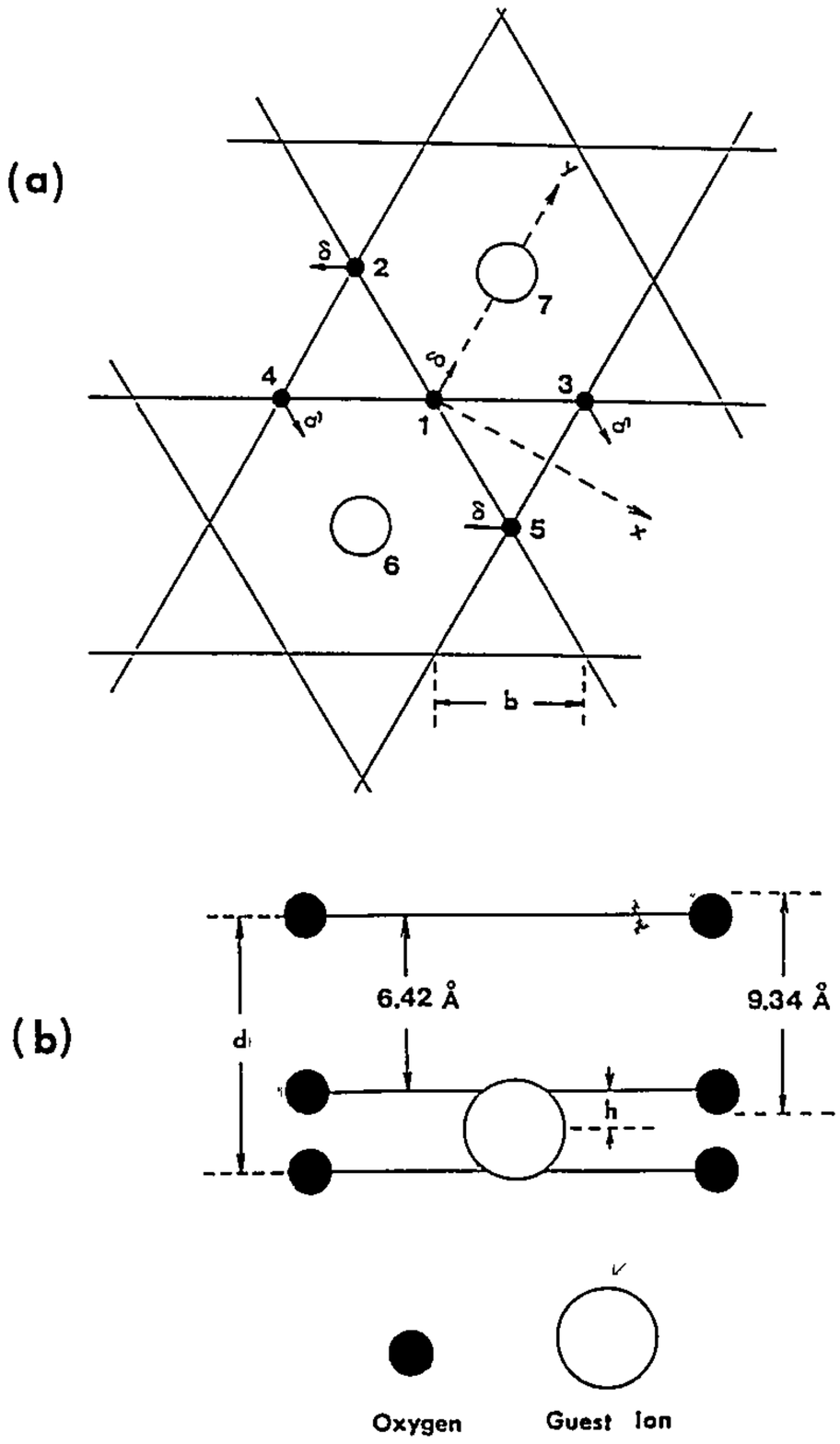

Figure 5. Configuration of oxygen atoms and guest ions of $A_{1-x}B_x$–V viewed in the direction (a) along and (b) perpendicular to the c-axis. The lattice parameter is $b = 2.67$ Å. $h = (d - 6.42)/2$ (Å) is the distance between the center of the guest ion in the gallery and the basal plane and d is the basal spacing. The arrows indicate the distorted positions of oxygen atoms in the torsional mode.

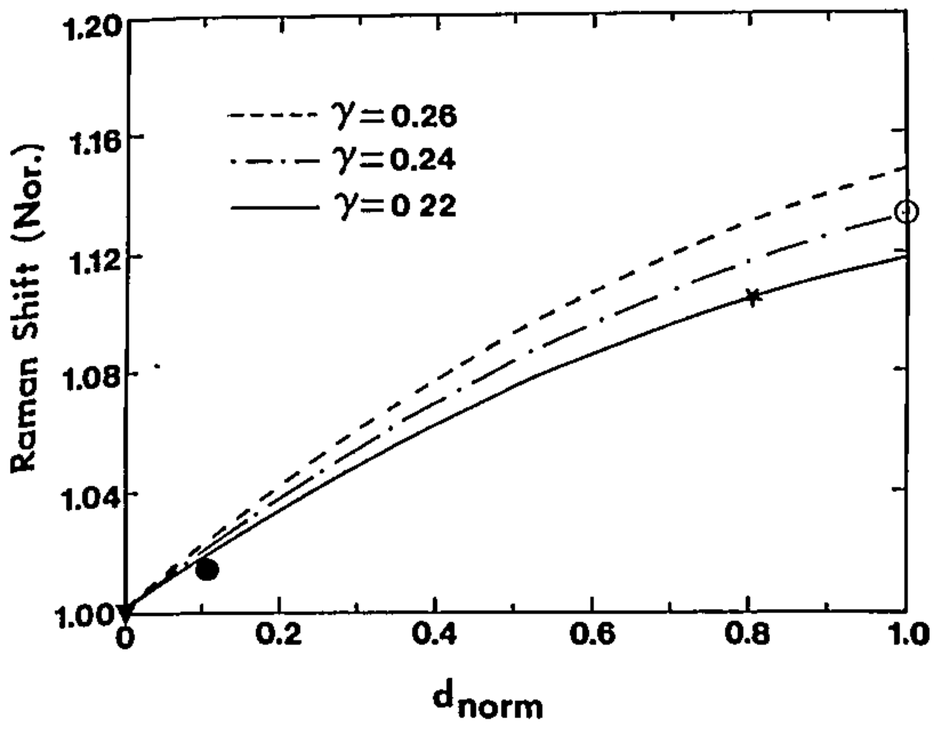

Figure 6. Calculation results [see Eqn (8)] of the normalized Raman shift of the torsional mode of M^+–V as a function of normalized basal spacing with three different ratios of force constants between oxygen–guest ion to oxygen–oxygen. The experimental results are shown with the same symbols as in Fig. 4.

results, we can calculate the force constant ratio γ. We can also calculate the Raman shift of the torsional mode as a function of basal spacing d, and of α and β. For the van der Waals type force, $n = -7$.

In Fig. 6, we plot from Eqn (8) the normalized Raman shift of the torsional mode, $\tilde{\nu}_{\text{norm}}$, as a function of the normalized basal spacing, d_{norm}, for three different values of γ. Here $d_{\text{norm}} = (d_{\text{obs}} - d_{\text{min}})/(d_{\text{max}} - d_{\text{min}})$, where d_{obs} is the observed basal spacing and $d_{\text{max}} = d_{(CH_3)_4N^+} = 13.3$ Å and $d_{\text{min}} = d_{\text{Rb}} = 10.23$ Å. The Raman shifts are normalized to the Raman frequency of Rb–V, that is, $\tilde{\nu}_{\text{norm}} = \tilde{\nu}/\tilde{\nu}_{\text{Rb}}$ with $\tilde{\nu}_{\text{Rb}} = 106\ \text{cm}^{-1}$. The reason we plotted $\tilde{\nu}_{\text{norm}}$ as a function of d_{norm} instead of $\tilde{\nu}$ *vs.* d directly is that we only have four groups of experimental data of d_i, $\tilde{\nu}_i$ [$i = 1$–4, corresponding to Rb^+–, Cs^+–, $(CH_3)_3NH^+$– and $(CH_3)_4N^+$–V], whereas there are five unknown parameters (α, β_i, $i = 1$–4). In Fig. 6, the symbols used are the same as in Fig. 5. The calculation results are in reasonable agreement with experiment, as can be seen from Fig. 6. For a fixed value of γ, the Raman shift of the torsional mode increases with basal spacing d. The force constant for the oxygen–guest ion interaction is of the order of 0.2–0.3 times that for the oxygen–oxygen interaction. The same method can also be used for other vibrational modes of CICs.

CONCLUSION

The Raman spectra of the torsional mode of $[(CH_3)_4N^+]_{1-x}[(CH_3)_3NH^+]_x$–V has been studied and the Raman frequency of this mode is larger than that of corresponding mode of $Cs_{1-x}Rb_x$–V. The x dependence of Raman shift of the torsional mode shows a shift to low energy with increasing x, but the x dependence of this mode for $[(CH_3)_4N^+]_{1-x}[(CH_3)_3NH^+]_x$–V is distinct from that of $Cs_{1-x}Rb_x$–V. By using the nearest neighbor approximation and assuming a van der Waals-type interaction force, we have calculated the Raman shift as a function of the basal spacing and the ratio of the force constants between oxygen–guest ions and oxygen–oxygen. The calculation results are consistent with the experimental observations. If the spatial distribution of guest ions in the interlayer space were known, we could in principle use the same methods as described above to calculate the Raman shift of the torsional mode of $A_{1-x}B_x$–V as a function of basal spacing in the region of $0 < x < 1$.

Acknowledgements

We gratefully acknowledge helpful discussions with S. Mahanti, S. Lee, W. Jin and Y. B. Fan. This work was supported by NSF–MRG Grant DMR 8903579 and in part by the Michigan State University Center for Fundamental Materials Research.

REFERENCES

1. B. R. York, S. A. Solin, N. Wada, R. Raythatha, I. D. Johnson and T. J. Pinnavaia, *Solid State Commun*. **54**, 475 (1985).
2. S. Lee, H. Kim, S. A. Solin and T. J. Pinnavaia, in *Chemical Physics of Intercalation*, edited by A. P. Legrand and S. Flandrois. Nato ASI, **172**, 497 (1987).
3. N. Wada, R. Raythatha and S. Minomura, *Solid State Commun*. **63**, 783 (1987).
4. R. E. Grim, *Clay Mineralogy*. McGraw-Hill, New York (1968), and references cited therein.
5. G. W. Brindly and G. Brown (Eds), *Crystal Structures of Clay Minerals and Their X-Ray Identification*. Minerological Society, London (1980).
6. R. Zallen, *The Physics of Amorphous Solids*, Chapt. 4. Wiley, New York (1983).
7. P. Wong, J. Howard and J. Lin, *Phys. Rev. Lett*. **57**, 637 (1986).
8. J. J. Fripiat (Ed.), *Advanced Techniques For Clay Mineral Analysis*. Elsevier, Amsterdam (1982).
9. T. J. Pinnavaia, *Science* **220**, 365 (1983).
10. S. A. Solin, P. Chow and H. Zabel, *Phys. Rev. Lett*. **53**, 1927 (1984).
11. S. A. Solin, *Adv. Chem. Phys*. **49**, 455 (1982).
12. H. C. Gupta, S. D. Mahanti and S. A. Solin, *Phys. Chem. Miner*. **16**, 291 (1988).
13. H. Kim and T. J. Pinnavaia, unpublished work.
14. J. Ishii, T. Shimanouchi and M. Nakahira, *Inorg. Chim. Acta* **1**, 387 (1967).
15. D. Billaud and A. Herold, *Bull. Soc. Chim. Fr*. **11**, 2404 (1974).
16. C. Kittel, *Introduction to Solid State Physics*, 5th ed., p. 79. Wiley, New York (1976).
17. C. Kittel, *Introduction to Solid State Physics*, 5th ed., p. 100. Wiley, New York (1976).